Using Lidar, in-situ measurements and Trajectory Analysis to observe air pollution in Beijing, 2014

Chen Zhenyi[1]*, Liu Wenqing[1], Liu Jianguo[1], Zhang Tianshu[1] and Dong Yunsheng[1]

*[1]Key Laboratory of Environmental Optical and Technology, Anhui Institute of Optics and Fine Mechanics, Chinese Academy of Sciences, Hefei, 230031, China, *Email: zychen@aiofm.ac.cn*

ABSTRACT

We present combined Mie lidar, ozone lidar and wide-range particle spectrometer observations that were carried out in Beijing, north China during two periods—one haze period before the Asia-Pacific Economic Cooperation (APEC) meeting and one moderate pollution period during the meeting in 2014. High extinction coefficient, moderate ozone concentration and variable particle number concentration were obtained throughout the first haze observation period. The mean extinction coefficients in the two pollution periods were 0.52 km-1 and 0.23 km^{-1}, respectively, at 532 nm. The ozone concentration during the first haze phase was more various with higher average value of 49 ppb compared to that in the second pollution observations (32 ppb). The comparison of aerosols and ozone in different heights indicate different pollution sources and complicated ozone process of generation and disappearance. The four-day back trajectories from a HYSPLIT model indicate that the air masses in the lower boundary layer were advected from the densely populated south regions of China and the long pollution transportation passing through northern China.

1. INTRODUCTION

Aerosol particles can absorb and scatter radiation efficiently, thereby affecting the balance of the atmospheric radiation system of the Earth [1-2].And many studies indicated that both direct emitted particles from human activities and secondary aerosols lead to significant reduction in visibility and the increase of haze occurrence [3-5]. Especially fine particles (PM2.5) suspended in the air may easily enter the respiratory and blood circulation systems and thus undermine human health [6]. Ozone is an important source of the hydroxyl radical, an oxidant that breaks down most pollutants and some greenhouse gases in the troposphere. Much of the present tropospheric ozone burden is also a consequence of anthropogenic emissions of ozone precursors resulting in widespread increases in ozone concentrations [7-8]. Thus it is important get understanding of aerosol properties and ozone concentration variation.

Thus far, some extensive studies using different methods have been conducted in the North China, with regard to aerosol pollution [9-11]. For example, *Tesche et al*. (2007) presented lidar observations of particle optical properties (backscatter coefficient, extinction coefficient and lidar ratio) in Beijing in North China. *Xue et al.* (2009) reports the results of the measurements of sulfur dioxide (SO_2) and aerosol scattering coefficient obtained from several aircraft campaigns during summer and autumn 2007 in the north-eastern regions of China. *Pan et al* (2013) measured trace elements of size-resolved aerosols at a rural site in North China and found the metallic episodes were attributable to the long-range transportation. Recently *Guo et al* (2014) illustrated the similarity and difference in particulate matter formation between Beijing and other world regions. However, knowledge on the combined optical properties of aerosol particles and ozone over northern China is particularly sparse, at least in the vertical scale. Therefore, experimental data in northern are strongly needed to assess the role of aerosols in future scenarios of global change and the impact on human health.

The paper is organized as follows: In Section 2 we describe the experimental setup (Mie lidar, ozone lidar and Wide-range Particle Spectrometer (WPS)). In Section 3, the metrological condition and in-situ measurements are presented. And aerosol optical properties and ozone profiles are shown along with the data interpretation. Furthermore the comparison between aerosol and ozone are investigated. Back trajectory analysis is

used to track the origin of the air mass arriving at our observation site and the aerosol sources. In Section 4 we provide conclusions based on the results in this experiment.

2. METHODOLOGY

2.1 532 Mie lidar

The 532Mie-backscattered lidar is made up of three sub-systems—emitting system, receiving system and signal analogue system. The laser source used is a pulsed Nd: YAG laser emitting short pulses at 532. The receiving telescope of the lidar system is based on a Cassegrainian design. The backscatter signal are then collected and focused on the telescope's focal point. After separating and passing the respective interference filters, the photons elastically backscattered at the 532 nm wavelengths are detected with photomultiplier tubes. After data preprocessing, the particle backscatter coefficient and the particle extinction coefficient at 532 nm could be retrieved by the Klett method.

2.2 Ozone DIAL

DIAL measurements of ozone in our system are made in the Hartley band with the on-line nominally set near 289 nm and the off-line set near 299 nm. And the pulsed light at wavelengths of 289 nm, 299 nm and 316 nm is generated by stimulated Raman scattering. Two lenses in front of and after the tube constitute a Raman con-focal system. The backscattered radiation from the atmosphere is collected by a 40 cm diameter telescope with an effective focal length of 400 cm. After passing through the field stop, the UV DIAL returns are reflected to a four-wavelength grating spectrometer. Both reflected beams are independently collimated to be compatible with interference filters and PMT areas. The resolution of ozone DIAL is 15 m under the height of 3km.

2.3 WPS

Particle Number Size Distribution (PNSD) in the size of 10 nm to 10 μm is measured by a Wide-range Particle Spectrometer (WPS^{TM} model 1000xp, MSP Corporation, USA). The WPS system consists of a Differential Mobility Analyzer (DMA), a Condensation Particle Counter (CPC) and a Laser Particle Spectrometer (LPS). CPC and LPS are utilized to measure PNSD ranged from 10-500 nm and 350 nm-10 μm respectively. The number concentration has a ± 10% error as indicated by the manufacturer. The instrument's time resolution was set at 5 min with 48 channels for each size for the DMA and 24 channels for the LPS.

3. RESULTS

3.1 In-situ Measurements

Figure 1 illustrates the time sequence plots of the aerosol extinction at 532nm measured by lidar during the observation period. Because of the incomplete overlap between the laser beam and the receiver field of view, only lidar measurements above 100m were subsequently used for the inversion. The lidar signals showed the enhanced pollution from October 28 to October 30 and from November 4 to November 5. More specifically, the median PM2.5 particle concentration reaches its maximum on October 30 and November 4 by the end of the afternoon (18–20 UTC) with the respective value of 100 ug/m^3 and 150 ug/m^3 (Figure 2). The highest NO concentration suggested the peak traffic in rush hours. This is due to the titration effect of ozone by freshly emitted NO from traffic in the city. And NO_2 mean concentration is high with value of 30 ppb and 50 ppb from October 29 to October 31 and from November 4 to November 5 respectively. Large NO_2 enhancements were observed in the noon of October 30 and November 4. Because the average value of the RH at ground level did not exceed 85% to reach saturation, we conclude that the two pollution periods: one haze pollution period from October 28 to October 30 and one moderate pollution period from November 4 to November 5.

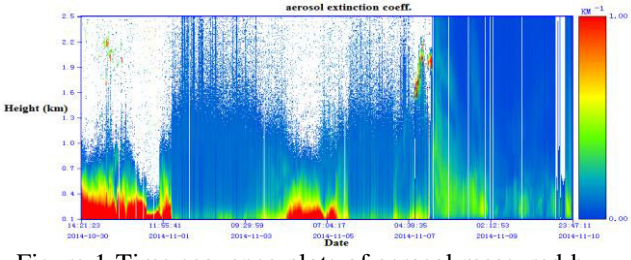

Figure 1 Time sequence plots of aerosol measured by lidar at 532 nm from October 30 to November 10, 2014

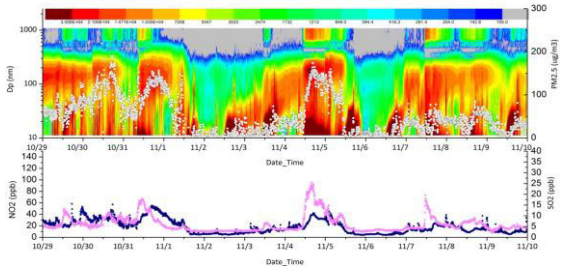

Figure 2 Variations of PM2.5 concentration, NO_2, SO_2 and PNSD from October 29 to November 10, 2014

3.2 Aerosols optical properties and ozone

The aerosol-ozone evolution and the aerosol loading impacts on ozone concentration are represented in Figure 5. During the first pollution period, the DIAL observations show pronounced a high ozone layer between 1 km and 2 km on October 29, with levels exceeding 60 ppb. The aerosol retrieval at 2 km (Figure 3(a)) indicates turbid air conditions below 2.5 km during the daytime and the average value of extinction coefficient is 0.52 km^{-1}. In the moderate pollution period, ozone concentration profile is less turbulent and maintains the average value of 32 ppb from 0.5 km to 2 km on November 4(Figure 3(b)).

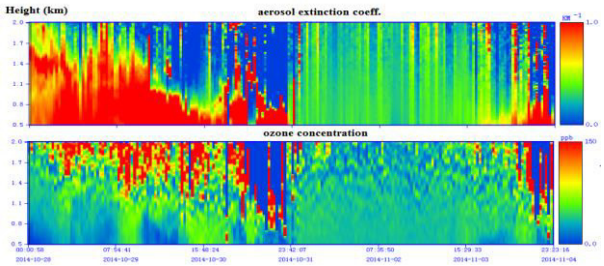

Figure 3 The aerosol-ozone evolution from October 28 to November 4, 2014

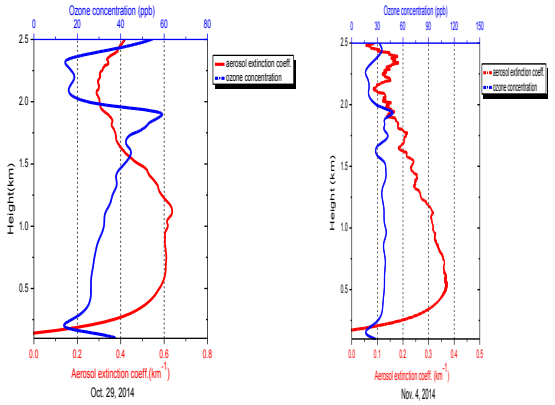

(a) (b)

Figure 4 Comparison of aerosol and ozone profiles on October 29 and November 4, 2014

In the two pollution episodes, aerosols show negative impacts on ozone concentrations on near ground level (from 100m to 200m) at all aerosol loading, which corresponds to the negative influence on photolysis rates by aerosols. However, positive impacts ozone concentrations in the lower troposphere (from 0.5 km to 2.5 km) are observed at small loadings for aerosols. Because in the upper troposphere where NOx is limited and net ozone destruction condition exists, a positive impact on photolysis rates causes a larger enhancement in ozone photo-dissociation rather than NO_2 photo-dissociation. *Lefohn et al.* [12] previously noted an increase in the low troposphere the probability distribution of ozone concentrations and attributed it to a decrease in NO emissions resulting in less effective titration. This positive correlation between ozone and aerosol in the troposphere on October 29 and November 4 suggests the same source is responsible for the enhanced ozone and aerosols.

3.3 Sources

During the first haze period (Figure 5(a)), the airflows from different directions at different heights began to converge in the J^3A since October 26. The air mass below 0.5 km was mainly from the densely populated southeast regions of China and the long pollution transportation passing through northern and northeast China. Straw burning and incomplete combustion of carbonaceous fuels during the heating period in winter is common and may cause more absorbing aerosols . The airflow dead zone made the diffusion more difficult. Thus, pollution accumulated and haze began to prevail.

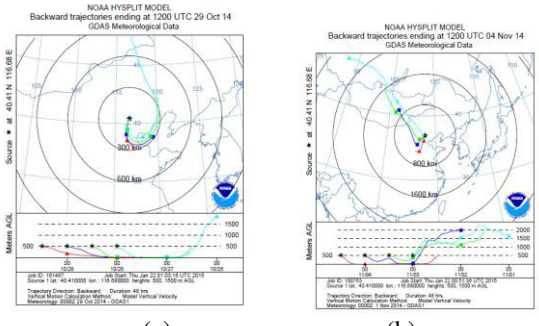

(a) (b)

Figure 5 Backward trajectories from HYSPLIT ensembles at 0.5km ending at Beijing, North China at 12:00 UTC on October 29 and November 4 2014

The air mass at 0.5km during the second pollution period was a bit different from that in the first haze period (Figure 9(b)); it came from southwest regions and northwest of China. The trajectories at 0.5 km showed the moderate pollution was due to the presence of more aerosol particles from adjacent region of southwest Beijing and the growth of aerosol under high relative humidity.

4. CONCLUSIONS

The results show the retrieval of aerosol extinction and ozone based on Mie lidar and ozone DIAL lidar measurements. Particle extinction coefficients were as large as 0.4 - 0.6 km-1 in the lower parts of the troposphere layer in the end of October 2014 in Beijing. And the ozone concentration maintained the high mean value of 49 ppb. Compared to the first pollution episode, the aerosol extinction coefficient in the second pollution period was smaller with decreased average value of 0.31km-1 and the ozone concentration was lower. The different aerosol and ozone peaks at different heights showed the different pollution sources, ambient meteorological conditions, and the resulting aerosol accumulation. And the backward trajectory indicates that both the short range and long range polluted air masses accumulated in the J^3A Beijing during the two pollution episodes.

ACKNOWLEDGEMENT

This work is supported by the project "Haze Observation Project Especially for Jing-Jin-Ji Area（HOPE-J3A，Grant No. KJZD-EW-TZ-G06-01）" of CAS. The authors also gratefully acknowledge the NOAA Air Resources Laboratory (ARL) for providing the HYSPLIT transport and dispersion model used in this research.

REFERENCES

[1] Bardouki H., Liakakou H., Economou C., Scaire J., Smolik J., V. Zdimal, 2003,Chemical composition of size resolved atmospheric aerosols in the Eastern Mediterranean during summer and winter, *Atmos. Environ.*, **37**, 195–208

[2] Ramanathan V. and Feng Y., 2009, Air pollution, greenhouse gases and climate change: Global and regional perspectives, *Atmos. Environ.*, **43**, 37–50

[3] Harrison R.G., Aerosol-induced correlation between visibility and atmospheric electricity, 2012, *J. Aerosol Sci.*, **52**, 121–126

[4] David Y.H. P., Chen S.C. and Zuo Z.L., 2014, PM2.5 in China: Measurements, sources, visibility and health effects, and mitigation, *Particuology*, **13**, 1-26

[5] Kessner A.L., Wang J., Levy R.C., Colarco P.R., 2013, Remote sensing of surface visibility from space: A look at the United States East Coast, *Atmos. Environ.*, **81**, 136–147

[6] Pope C.A., Thun M.J., Namboodiri M.M., Dockery D.W., Evans J.S., Speizer F.E., 1995, Particulate air pollution as a predictor of mortality in a prospective study of U.S. adults, *AM J RESP CRITCARE*, **151**, 669–674

[7] Shi C.Z., Wang S.S., Liu R., Zhou R., Li D.H, Wang W.X., Li Z.Q., Cheng T.T. and Zhou B., 2015, A study of aerosol optical properties during ozone pollution episodes in 2013 over Shanghai, China, *Atmos. Res.* , **153**, 235–249

[8] Hoshika Y., Watanabe W., Kitao M., Häberle K.H., Grams T. E.E., Koike T. and Matyssek R., 2015, Ozone induces stomatal narrowing in European and Siebold's beeches: A comparison between two experiments of free-air ozone exposure, *Environ. Pollut.*, **196**, 527-533

[9] Xue L.K., Ding A. J., Gao J., Wang T. , Wang W.X., Wang X.Z., Lei H.C., Jin D.J and Qi Y.B., 2010,Aircraft measurements of the vertical distribution of sulfur dioxide and aerosol scattering coefficient in China, *Atmos. Environ.*, **44**, 2, 278–282

[10] Pan Y.P., Wang Y.S., Sun Y., Tian S.L. and Cheng M.T, 2013, Size-resolved aerosol trace elements at a rural mountainous site in Northern China: Importance of regional transport, *Sci. Total Environ.*,461–462

[11] Guo S., Hu M., Zamora M. L., Peng J.F., Shang D.J., Zheng J., Du Z.F., Wu Z.J., Shao M., Zeng L.M., Molina M. J. and Zhang R.Y., 2014, Elucidating severe urban haze formation in China, *PNAS*,111 ,**49** , 17373–17378

[12] Lefohn, A. S., Shadwick, D. and Oltmans, S. J., 2008,Characterizing long-term changes in surface ozone levels in the United States (1980–2005). *Atmos. Environ.*, **42**, 8252–8262